Synthesis and antitumoral activity of novel biaryl hydroxy-triazole and fluorene-triazole hybrids

David Chafi Zeitune[1†] , Marcelo Folhadella Martins Faria Azevedo[1†] , Mariane Senna Rangel[1], Robert de Sousa Bastos[2] , José de Brito Vieira Neto[2] , Claudia do Ó Pessoa[2,3] , Camilla Djenne Buarque[1*]

[1]Department of Chemistry, Pontifical Catholic University of Rio de Janeiro (PUC-Rio), Rio de Janeiro 22451-900, Brazil
[2]Núcleo de Pesquisa e Desenvolvimento de Medicamentos (NPDM), Federal University of Ceará (UFC), Fortaleza 60430-275, Brazil
[3]Department of Physiology and Pharmacology, Universidade Federal do Ceará, Fortaleza 60430-275, Brazil

[†]These authors contributed equally to this work.
*Correspondence: Camilla Djenne Buarque, Department of Chemistry, Pontifical Catholic University of Rio de Janeiro (PUC-Rio), Rio de Janeiro 22451-900, Brazil. camilla-buarque@puc-rio.br
Academic Editor: Fernando Albericio, University of KwaZulu-Natal, South Africa, Universidad de Barcelona, Spain
Received: December 31, 2024 **Accepted:** March 26, 2025 **Published:** April 21, 2025

Abstract

Aim: The development of selective and potent antitumor agents remains a significant challenge. This study aimed to synthesize and evaluate biaryl hydroxy-1,2,3-triazoles and 9*H*-fluorene-1,2,3-triazole hybrids, inspired by previously identified bioactive 1,2,3-triazoles, for their cytotoxic potential against human cancer cell lines.

Methods: A library of 13 biaryl hydroxy-1,2,3-triazoles and 11 fluorene-1,2,3-triazoles was synthesized using optimized Suzuki and telescopic one-pot reactions, with yields ranging from 16% to 97%. The cytotoxicity of these compounds was tested against HCT-116 (colorectal cancer), SNB-19 (astrocytoma), MDA-MB-231 (triple-negative breast cancer), and MOLM-13 (acute myeloid leukemia, FLT3-ITD mutant) cell lines.

Results: Two fluorene-triazoles, 1-(2-bromophenyl)-4-(9*H*-fluoren-9-yl)-1*H*-1,2,3-triazole (LSO258) and 1-(4-bromophenyl)-4-(2-fluoro-9*H*-fluoren-9-yl)-1*H*-1,2,3-triazole (LSO272), both containing bromine substituents, exhibited selective cytotoxicity against MOLM-13, with half-maximal inhibitory concentration (IC$_{50}$) values of 25.5 μM and 12.5 μM, respectively. Furthermore, LSO258 and LS0272 showed a selectivity index ≥ 2 towards the MOLM-13 cell line. Biaryl hydroxy-1,2,3-triazoles displayed broader activity, with [1,1'-biphenyl]-2-yl(1-(2,5-dibromophenyl)-1*H*-1,2,3-triazol-4-yl)methanol (LSO278), featuring two bromine groups, demonstrating potency across HCT-116, MDA-MB-231, and MOLM-13 (IC$_{50}$: 23.4 μM, 34.3 μM, and 18.7 μM, respectively). However, structural rigidity did not consistently predict activity, as 1-(2,5-dibromophenyl)-4-(9*H*-fluoren-9-yl)-1*H*-1,2,3-triazole (LSO275), a rigid fluorene-triazole, was inactive. MOLM-13 was the most sensitive cell line, with compounds such as 4-(9*H*-fluoren-9-yl)-1-(4-(trifluoromethyl)phenyl)-1*H*-1,2,3-triazole (LSO259) and (1-(4-bromophenyl)-1*H*-1,2,3-triazol-4-yl)(4'-

fluoro-[1,1'-biphenyl]-2-yl)methanol (LSO280), achieving maximum growth inhibition (MGI > 55%) despite not reaching IC_{50} values.

Conclusions: The results highlight the critical role of bromine substitution on the aryl azide-derived ring in modulating cytotoxic activity. The study reinforces the potential of rigid fluorene-based scaffolds as promising leads for the development of targeted therapies against FLT3-mutant leukemia, aligning with previous reports on 1,2,3-triazole hybrids antiproliferative activity in leukemia models.
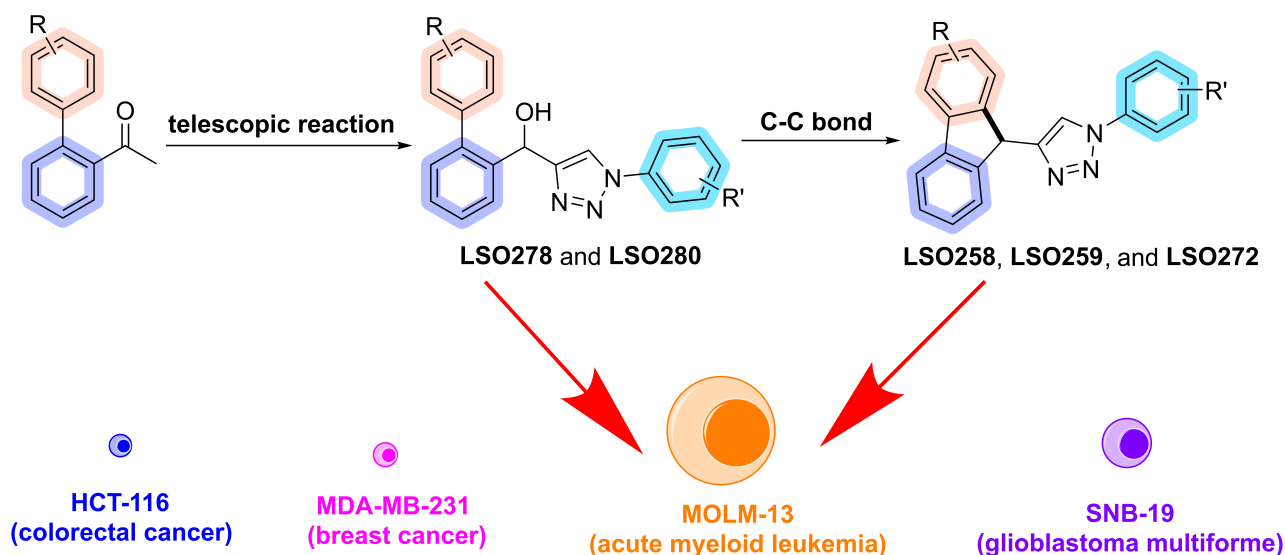
Graphical abstract. Hydroxy-triazole and fluorene-triazole hybrids and their antitumoral activity

Keywords

1,2,3-Triazole, 9*H*-fluorene, cycloaddition, enaminone, leukemia, cancer

Introduction

Cancer has become the leading cause of death worldwide among people under 70 years old [1]. In addition, premature deaths due to various types of cancer are also rising across countries [2]. In 2020, the estimated number of cancer cases was almost 20 million, and 10 million deaths related to cancer. Among the most common and fatal cancers include breast, prostate, lung, colon, and leukemia [3]. Cancer cells are constantly evolving which results in a high tumor heterogeneity with a subpopulation of cells displaying a different molecular landscape [4]. This characteristic leads to drug resistance due to genetic, epigenetic, and metabolic changes that hinder anticancer activity [5, 6]. Another important factor that limits cancer treatment is chemotherapy-related toxicities that affect healthy cells leading to acute toxicities, such as hematological and gastrointestinal [7, 8]. Therefore, there is an urgent need for the development of new anticancer compounds to overcome these limitations.

Among the most promising scaffolds for addressing challenges in cancer therapy are 1,2,3-triazoles, a class of heterocycles known for their exceptional stability and diverse pharmacological properties. Their mechanisms of action include the inhibition of cancer cell proliferation, cell cycle arrest, and induction of apoptosis, making them effective against both drug-sensitive and multidrug-resistant cancers [9].

In recent years, triazole-based hybrid compounds have emerged as promising candidates for cancer treatment, demonstrating remarkable therapeutic potential [10]. These hybrids often exhibit dual or multiple mechanisms of action, addressing the limitations of conventional chemotherapeutics by improving selectivity and reducing side effects. Furthermore, their ability to overcome drug resistance and their promising in vivo activities against various cancer types have solidified their role as valuable frameworks

for next-generation anticancer agents. By integrating triazoles into hybrid molecules, researchers aim to unlock new possibilities for more effective and safer cancer therapies [11].

Aryl(1-aryl-1*H*-1,2,3-triazole-4-yl)methanols, commonly known as hydroxy-1,2,3-triazoles, are a promising and versatile scaffold with significant potential for novel drug development. Our research group has extensive expertise in their synthesis, utilizing both copper-catalyzed alkyne-azide cycloaddition (CuAAC) between propargylic alcohols and aryl azides [12], as well as the metal-free and solvent-free enaminone-azide cycloaddition (EACA) employed in this study to synthesize 4-acyl-1,2,3-triazoles [13]. The EACA method provided a simpler and more efficient route to generate bioactive hydroxy-1,2,3-triazoles through acyl reduction. These compounds presented antileishmanial [14], antiviral [15], and cystic fibrosis activity [13].

9*H*-Fluorene-based compounds have emerged in past years due to their unique chemical and physical properties, which allow their application in a wide range of scientific disciplines, such as optoelectronics [16, 17], solar cells [18], nanostructures [19, 20], and others. Its great prominence is seen in the field of medicinal chemistry where this scaffold is being used in various bioactive compounds [21–24].

Given their structural characteristics (conformational rigidity with significant aromaticity structure), which intensify their pharmacophoric characteristics [25, 26], it is possible to combine them with other structures, such as 1,2,3-triazoles. These synthetic heterocycles have great potential and applicability, mainly due to their trans-amides bioisosteric proprieties that possess broad-spectrum biological activity, low cytotoxicity, and significant structural versatility. These properties allow triazoles to act both as pharmacophores, directly engaging biological targets, and as linkers in hybrid molecules, tethering different pharmacophores to enhance efficacy.

The development of fluorene-triazole hybrid compounds is a little-explored field with great potential. In literature, some examples are present so far, mainly in functional materials chemistry [27–31]. With a view to biological applications, examples can be found, however, most of them bonded together by fluorene's aromatic rings [32–35].

Fewer examples are found when it comes to 9*H*-fluorenes-triazole hybrids. Yang et al. [36] proposed the synthesis of fluorene-triazoles containing the pentafluorosulfanyl group, with emphasis on the CuAAC between 3,5-bis(pentafluorosulfanyl)phenyl azide (**1a**) and 9-ethynyl-9*H*-fluoren-9-ol (**2**) as presented in Figure 1a. The authors verified the ability of compound **3** to trigger cell death in human leukemic monocyte lymphoma U937 cells obtaining a half-maximal inhibitory concentration (IC_{50}) value of 6.29. Compound **3** was also compared to Caspase-3, an important enzyme responsible for apoptosis, which has been proven to be 3.4 times more efficient than this enzyme. These results demonstrate the antitumor potential of fluorene-triazole hybrids.

Looking for analogs of structures reported in the literature as *Mycobacterium tuberculosis* (*M. tb*) InhA (NADH-dependent 2-*trans*-enoyl-acyl carrier protein reductase) inhibitors, Suresh et al. [37] rationalized such molecular skeletons as essential elements for InhA inhibition. In this way, the authors presented three 9*H*-fluorene structures derived from fluorene-triazoles (**5**) with a good variety of substituents by reacting fluorene-based alkynes (**4**) and azidobenzenes (**1**) [37] (Figure 1b).

More recently in 2020, our research group reported 3 examples of 9*H*-fluorenes-triazole hybrids employing a Friedel-Crafts alkylation. Starting from substituted biaryl hydroxy-1,2,3-triazoles (**6**) (previously synthesized by CuAAC between biaryl-propargyl alcohols and azidobenzenes), in the presence of $Pd(OAc)_2$, Na_2CO_3, $PhI(TFA)_2$ in dichloroethane, 100°C for 36 hours, with yields of 25 to 40% [38] (Figure 1c). Since the metal-free and solvent-free EACA to obtain 4-acyl-1,2,3-triazoles is a simpler and more effective alternative than CuAAC, our research group decided to employ this methodology for obtaining biaryl hydroxy-1,2,3-triazoles (**6**) as precursors of 9*H*-fluorene-triazole (**7**) (Figure 1d). Given the biological potential of these compounds, another goal was to evaluate the antitumor potential by maximum growth inhibition (MGI) of the new biaryl hydroxy-1,2,3-triazoles and fluorene-triazole hybrids against different cell lines.
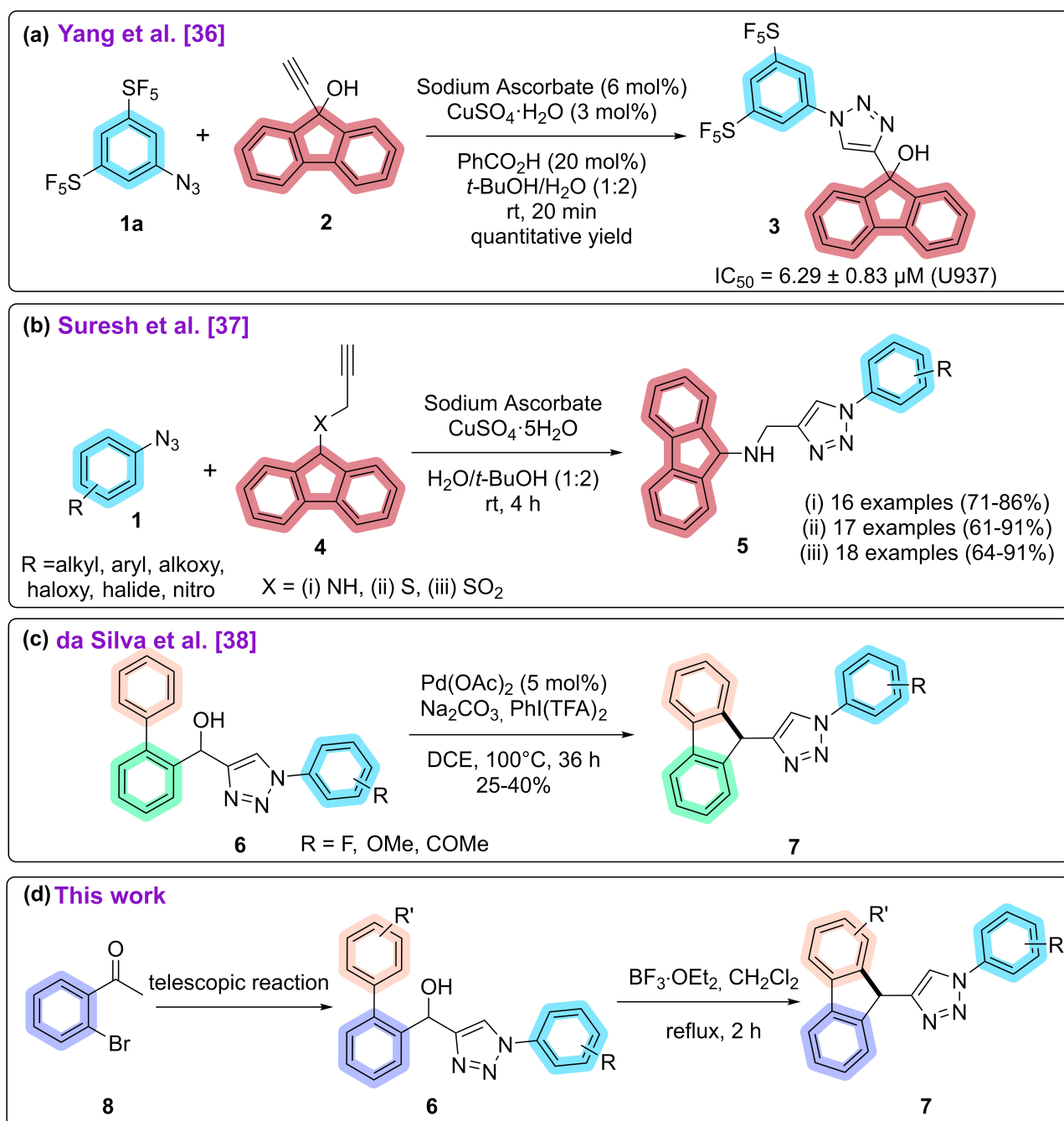
Figure 1. Summary of 9*H*-fluorene-1,2,3-triazoles hybrids. (**a**) Synthesis of fluorene triazoles according to Yang et al. [36]. (**b**) Synthesis of fluorene triazoles according to Suresh et al. [37]. (**c**) Synthesis of fluorene triazoles according to da Silva et al. [38]. (**d**) This work. DCE: 1,2-dichloroethane. rt: room temperature

Materials and methods

General procedure for the synthesis of biaryl acetophenones

In a 25 mL screw-top test tube, 2-bromoacetophenone (**8**) (0.199 g, 1.00 mmol), phenylboronic acid (**9**) (2.00 mmol), K_2CO_3 (0.276 g, 2.00 mmol), Pd(PPh$_3$)$_4$ (0.05 mmol) and 2.0 mL of water were added. The reaction was stirred constantly for 3 hours at reflux temperature under an argon atmosphere (Figure 2). At the end of the reaction, the organic phase was extracted with ethyl acetate (EtOAc), dried with anhydrous sodium sulphate (Na_2SO_4) and filtered through celite. The solvent was evaporated under reduced pressure and the product (**10**) was purified by flash column chromatography using EtOAc/hexane (10:90) as the eluent.
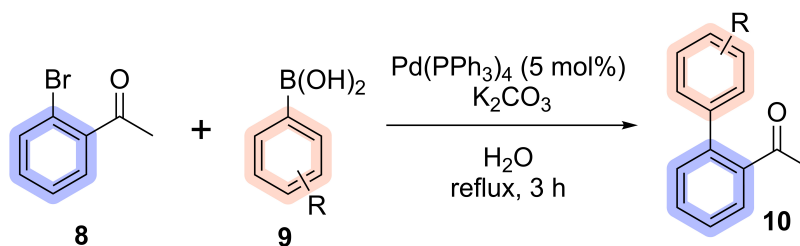
Figure 2. General procedure for the synthesis of biaryl acetophenones

General procedure for the synthesis of biaryl-acyl-1,2,3-triazoles

In a 25 mL screw cap test tube, biaryl acetophenone (**10**) (1.00 mmol), aryl azide (**1**) (1.50 mmol), and *N,N*-dimethylformamide dimethyl acetal (DMF-DMA) (0.238 g, 2.00 mmol) were added. The reaction was stirred constantly for 2 hours at 150°C under an argon atmosphere (Figure 3). At the end of the reaction, the product (**11**) precipitated pure in ice-cold ethanol and vacuum filtered.
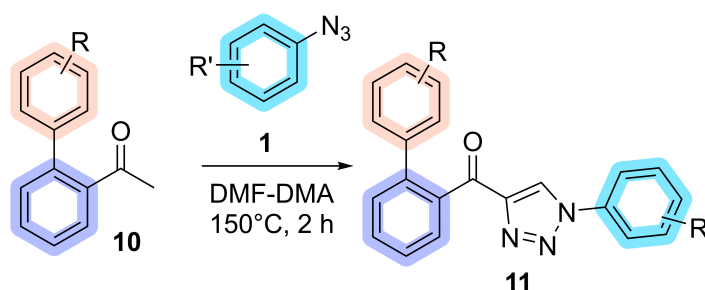

Figure 3. General procedure for the synthesis of biaryl-acyl-1,2,3-triazoles. DMF-DMA: *N,N*-dimethylformamide dimethyl acetal

General procedure for the synthesis of biaryl hydroxy-1,2,3-triazoles

Adapting the methodology from Azevedo et al. [13], starting with the addition of biaryl acetophenone (**10**) (1.00 mmol), aryl azide (**1**) (1.50 mmol), and DMF-DMA (0.238 g, 2.00 mmol) in a 25 mL screw-capped test tube the reaction was stirred constantly for 2 hours at 150°C under an argon atmosphere. Followed by the evaporation of the DMF-DMA, the tube was then cooled to room temperature, and NaBH$_4$ (0.151 g, 4.00 mmol) and 2.5 mL of methanol were added. The reaction was stirred constantly for 2 hours at reflux temperature (Figure 4). At the end of the reaction, the product (**6**) was filtered into ice-cold ethanol or extracted with EtOAc followed by purification via flash column chromatography using EtOAc/hexane (50:50) as the eluent.
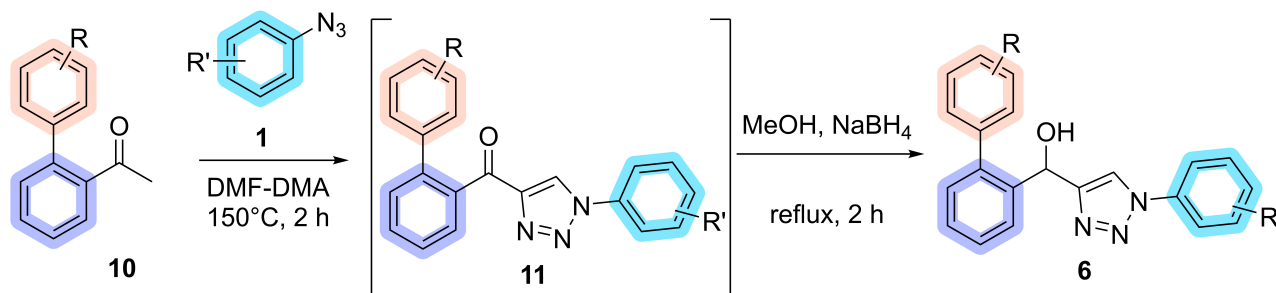

Figure 4. General procedure for the synthesis of biaryl hydroxy-1,2,3-triazoles. DMF-DMA: *N,N*-dimethylformamide dimethyl acetal

General procedure for the synthesis of 9*H*-fluorene-1,2,3-triazoles

In a 4 mL vial, biaryl hydroxy-1,2,3-triazole (**6**) (0.125 mmol), BF$_3$·OEt$_2$ (0.050 mL, 0.40 mmol) and 2.0 mL of dichloromethane were added. The BF$_3$·OEt$_2$ was added slowly in an ice bath under constant stirring, then

the reaction was brought to reflux temperature and continued for 2 hours (Figure 5). At the end of the reaction, the solvent was evaporated under reduced pressure and the product (**7**) was purified by column flash chromatography using EtOAc/hexane (10:90) as eluent.
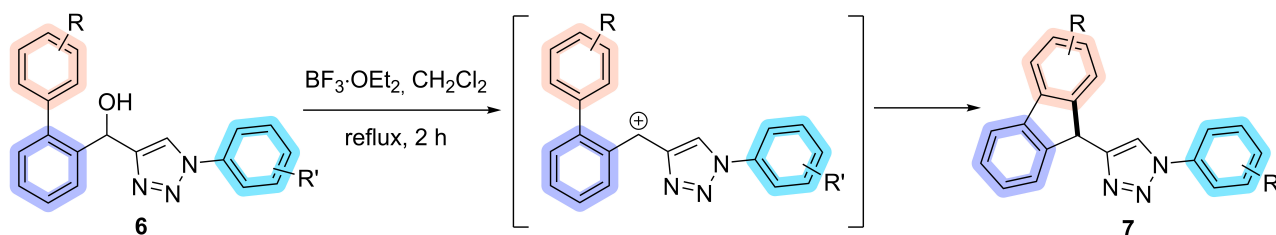

Figure 5. General procedure for the synthesis of 9*H*-fluorene-1,2,3-triazoles

Biological evaluation

Cell culture

Cell lines were obtained from the National Cancer Institute (Bethesda, MD). All cell culture media (Gibco™, Thermo Fisher Scientific, Cat. No. 31800022) contained 10% fetal bovine serum (Gibco™, Thermo Fisher Scientific, Cat. No. 12657029) and 1% penicillin/streptomycin (Gibco™, Thermo Fisher Scientific, Cat. No. 15140122). For the experiments, cells were seeded in 96-well plates (Nest™, Wuxi NEST Biotechnology, Cat. No. 701001) in the following concentrations 7×10^4 cells/mL (HCT-116), 2×10^5 cells/mL (MDA-MB-231), 1×10^5 cells/mL (MOLM-13 and SNB-19), and 1.5×10^5 cells/mL (HEK-293) and cells were maintained at 37°C with 5% CO_2 in a humidified incubator.

Maximum growth inhibition

The effects of biaryl hydroxy-triazoles and fluorene-triazoles compounds on human cancer cell viability, expressed as the percentage of cell growth inhibition, were determined by the MTT (3-(4,5-dimethyl-2-thiazolyl)-2,5-diphenyl-2*H*-tetrazolium bromide) (PerkinElmer, VICTOR Nivo Multimode Plate Reader, Waltham, MA). Colorimetric assay, as previously described [39, 40]. Cells were grown in 96-well plates (Vetec™, Sigma-Aldrich, Cat. No. V900888) at defined concentrations and exposed to a single concentration of 50 µM for 72 h. The negative control was treated with 0.5% DMSO (ACS™, ACS científica, São Paulo, BR). Afterward, the plates were centrifuged, and the medium was replaced by fresh medium (150 µL) containing 0.5 mg/mL MTT. Three hours later, the MTT formazan product was dissolved in 150 µL DMSO, and absorbance was measured using a multiple reader (PerkinElmer, VICTOR Nivo Multimode Plate Reader, Waltham, MA). Compound effect was quantified as the percentage of control (DMSO 0.5%) absorbance of the reduced dye at 595 nm. The compounds with MGI ≥ 75% in at least one human cancer cell line were selected for IC_{50} evaluation.

Antiproliferative effect IC_{50} evaluation

The IC_{50} evaluation of the selected fluorene-triazole hybrids was determined by the MTT colorimetric assay, as previously described [39, 40]. The research aimed to assess the IC_{50} of 5 compounds on four different human cancer cell lines: MOLM-13 [acute myeloid leukemia (AML)], SNB-19 (astrocytoma), MDA-MB-235 (breast cancer), HCT-116 (colon carcinoma cell line) and one non-tumor cell line, HEK-293 (human embryonic kidney). The tested compounds were dissolved in DMSO, and then added to each well, followed by incubation of 72 h at concentrations ranging from 0.4 to 50 µM. The negative control was treated with 0.5% DMSO. Afterward, the plates were processed as described above. Experiments were carried out in triplicate and repeated at least three times. The experiments were analyzed by linear regression using the GraphPad Prism program, version 6.01, to determine each IC_{50} value.

The selectivity index (SI) is based on the IC_{50} obtained for each cell line by calculating the ratio of IC_{50} on the non-cancer cell line over the IC_{50} for the cancer cell line. A compound is considered selective towards a tumor cell line with a SI ≥ 2 [41, 42].

$$SI = IC_{50}^{\text{non-cancer cells}} / IC_{50}^{\text{cancer cells}}$$

Results

Chemistry

Given that the most bioactive compounds for leishmaniosis and cystic fibrosis identified by our research group, such as (4-bromophenyl)(1-(4-bromophenyl)-1H-1,2,3-triazol-4-yl)methanol and (2-bromophenyl)(1-(4-bromophenyl)-1H-1,2,3-triazol-4-yl)methanol, feature bromine in the aryl ring derived from aryl azide, we designed biaryl hydroxy-1,2,3-triazoles and fluorene derivatives to incorporate the bromine group. So, we started exploring the Suzuki reaction using 2-bromoacetophenone as a substrate to obtain biaryl acetophenone **10a**.

The reaction, conducted under the conditions detailed in Table 1, entry 1, and adapted from the methodology reported by da Silva et al. [38], yielded the desired product in 65% yield after purification via column chromatography. To further optimize the reaction, different catalysts were evaluated in entries 2 and 3. Among the tested catalysts, $Pd(PPh_3)_4$ delivered the highest yield and was selected for subsequent studies. The next phase of optimization targeted the solvent and reaction time. With the reaction time fixed at 3 hours, various solvents were tested, including toluene, $EtOH:H_2O$ mixtures (20% and 50% ethanol), pure H_2O, and solvent-free conditions. Both $EtOH:H_2O$ mixtures and pure water exhibited comparable performance. Pure water was ultimately chosen due to its significant advantages in environmental sustainability, safety, and cost efficiency [43, 44].

Table 1. Reaction conditions optimization for the Suzuki reaction on 2-bromoacetophenone

Reaction for the Suzuki reaction on 2-bromoacetophenone	Entry	Catalyst	Solvent	Temperature	Time (h)	Yield (%)
	1	$Pd(OAc)_2$ + PPh_3[a]	Toluene	Reflux	16	65
	2	$PdCl_2$[b]	Toluene	Reflux	16	65
	3	$Pd(PPh_3)_4$[b]	Toluene	Reflux	16	80
	4	$Pd(PPh_3)_4$[b]	20% $EtOH:H_2O$	Reflux	3	90
	5	$Pd(PPh_3)_4$[b]	50% $EtOH:H_2O$	Reflux	3	93
	6	$Pd(PPh_3)_4$[b]	H_2O	Reflux	3	92
	7	$Pd(PPh_3)_4$[b]	-	200°C	3	70
	8	**$Pd(PPh_3)_4$[c]**	**H_2O**	**Reflux**	**3**	**95**
	9	$Pd(PPh_3)_4$[d]	H_2O	Reflux	3	60
	10	$Pd(PPh_3)_4$[c, e]	H_2O	Reflux	3	87

[a] Catalyst: 10 mol% and 20 mol% respectively. [b] Catalyst: 10 mol%. [c] Catalyst: 5 mol%. [d] Catalyst: 1 mol%. [e] Scale up to 10 mmol from 0.2 mmol. -: no solvent

The optimized conditions identified in Table 1, entry 8, emerged as the most efficient and reliable for the synthesis, using 5 mol% $Pd(PPh_3)_4$ in water as the solvent under reflux for 3 hours, achieving yields of 95%. To further validate their robustness and scalability, the reaction was performed on a 50-fold scale, maintaining excellent efficiency with a slightly reduced yield of 87% after purification. From this optimized condition, it was possible to synthesize 6 biaryl acetophenones, with yields ranging from 39 to 99%, as shown in Figure 6.
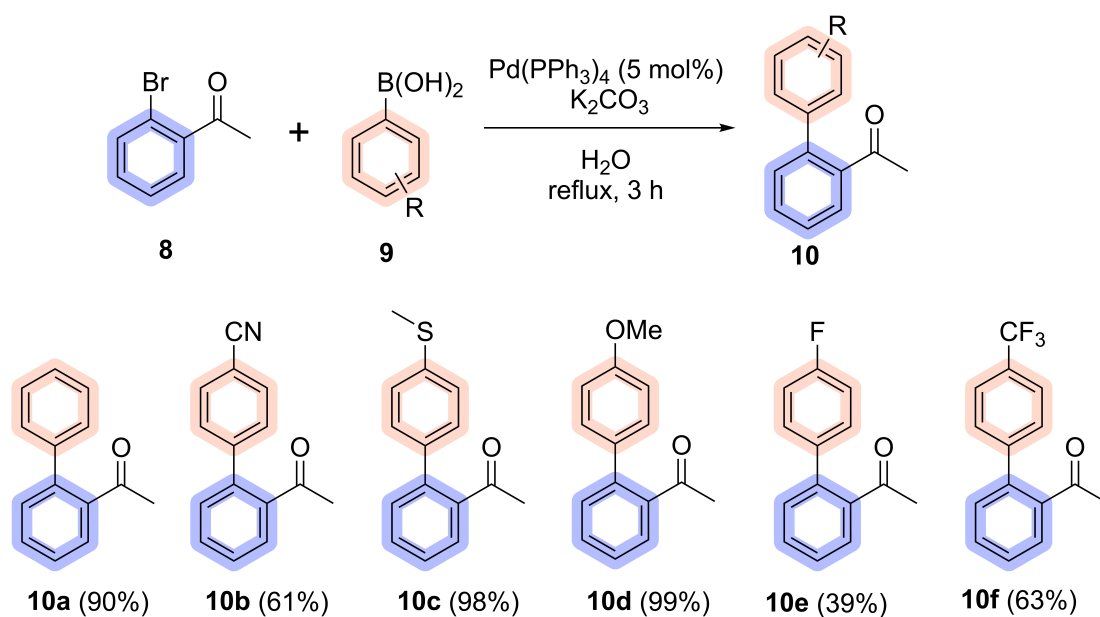
Figure 6. Scope of biaryl acetophenone at 1 mmol scale

According to the literature, in general, electron-rich organoboranes and electron-deficient halides are the most reactive substrates for the Suzuki reaction, thus resulting in a positive effect on the reaction yield [45, 46]. Given that the halide used is 2-bromoacetophenone, characterized by the presence of an electron-withdrawing group, and based on the scope presented above, the good yields obtained are in line with the trends reported in the literature. Additionally, boronic acids bearing electron-donating substituents consistently led to higher yields compared to those with electron-withdrawing groups, further corroborating established reactivity patterns.

The subsequent step involved applying the substituents previously established by the methodology for synthesizing 4-acyl-1,2,3-triazoles (**11**) from acetophenones and aryl azides [13]. The biaryl acetophenone **10a** reacted with 4-bromophenyl azide **1b** and DMF-DMA at 150°C for 2 hours. The mechanism for this reaction is a combination of previously described mechanisms for enaminone formation by Thomas et al. [47], as well as a mechanism described by the research group in 2022 [48]. This reaction successfully yielded the biaryl-acyl-1,2,3-triazole **11ab**, which was isolated in 40% yield following precipitation in ice-cold ethanol, with the NMR spectra corresponding to these molecules available in the supplementary material (Figures S1 and S2). The reduction of compound **11ab** was carried out using $NaBH_4$ in methanol under reflux for 2 hours. This reaction yielded the biaryl hydroxy-1,2,3-triazole **6ab** with complete conversion of the starting material (Thin Layer Chromatography-determined). The hydroxy-triazole precipitated directly from the reaction mixture upon the addition of water and was isolated by filtration, affording a yield of 93% (Figure 7).
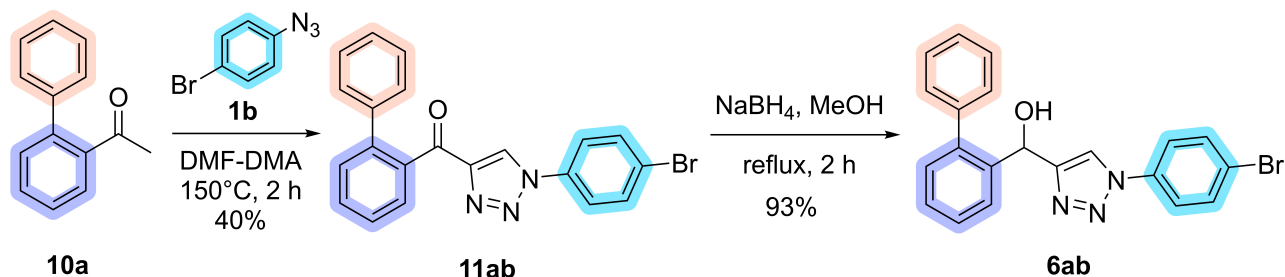

Figure 7. Synthesis of biaryl-acyl-1,2,3-triazole 11ab and biaryl hydroxy-1,2,3-triazole 6ab. DMF-DMA: *N,N*-dimethylformamide dimethyl acetal

Attempts to synthesize hydroxy-triazoles with other substituents revealed a significant limitation during the isolation of the acyl-triazoles. Unlike the previous case, none of the type **6** triazole precipitated in pure form, necessitating purification via column chromatography. The isolation process was further complicated by the similar retention factors of the **11** and the corresponding **10**, making their separation particularly challenging.

To address this challenge, a telescopic approach was proposed, applying the known properties of hydroxy-triazoles, which readily precipitate in pure form upon the addition of water. This one-pot methodology involved the in situ generation and consumption of intermediates, eliminating the need to isolate the acyl-triazole [49]. After evaporating DMF-DMA, the acyl group was directly reduced, enabling the synthesis of hydroxy-triazoles without requiring purification of the intermediate. Using the new telescopic approach, a diverse set of 13 novel biaryl hydroxy-1,2,3-triazoles (**6**) was successfully synthesized by varying the biaryl acetophenones and aryl azides, obtaining yields ranging from 16% to 89% ([Figure 8](#)).
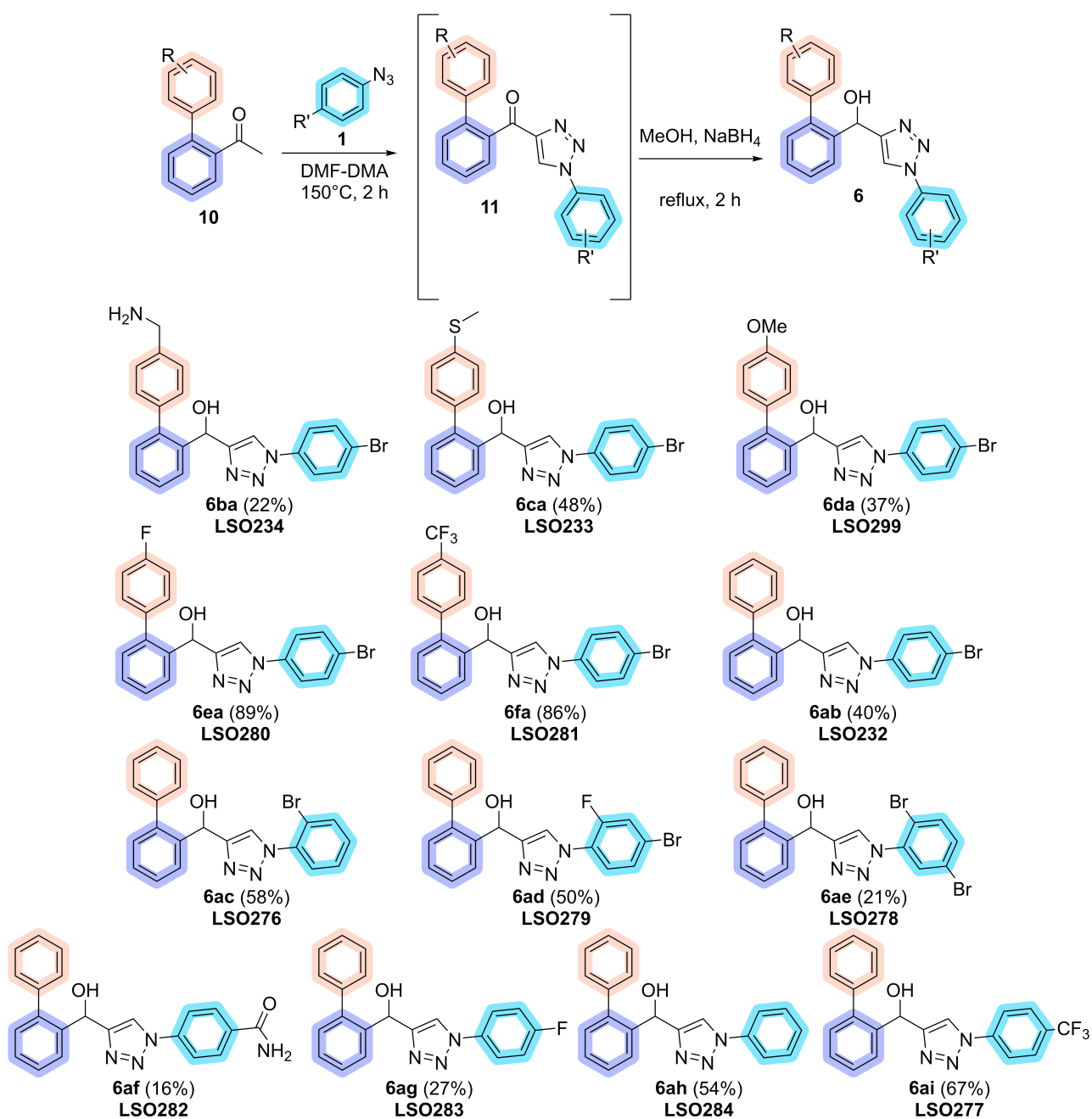

Figure 8. Scope of biaryl hydroxy-1,2,3-triazoles. DMF-DMA: *N,N*-dimethylformamide dimethyl acetal

The yields obtained showed significant variability, likely influenced by challenges in the synthesis of compound **11**, particularly the in situ formation of the enaminone, which is essential for its subsequent reaction with the azide to produce the triazole. Additionally, variations in the solubility of the reduced product during precipitation may contribute to inconsistencies in the final yield.

Once the bi-arylated precursors were synthesized, a methodology was required to access the desired fluorene-triazoles (**7**) boron trifluoride (BF$_3$) was selected due to its strong Lewis acid character, which effectively coordinates with and activates the secondary alcohol, facilitating the formation of the carbocation intermediate. This method not only allows for the use of mild reaction conditions but is also commercially available, easy to handle under standard laboratory conditions, and can be conveniently removed after the reaction, thereby streamlining the overall process [50–52].

The formation of fluorene was achieved via an intramolecular Friedel-Crafts alkylation approach with a carbocation as an intermediate [53]. This methodology was applied to biaryl hydroxy-1,2,3-triazoles, which were reacted with BF$_3$·OEt$_2$ in dichloromethane under reflux for 2 hours. Upon completion of the reaction, the solvent was evaporated, yielding 11 new 9*H*-fluorene-1,2,3-triazole in 20 to 97% yield (Figure 9).
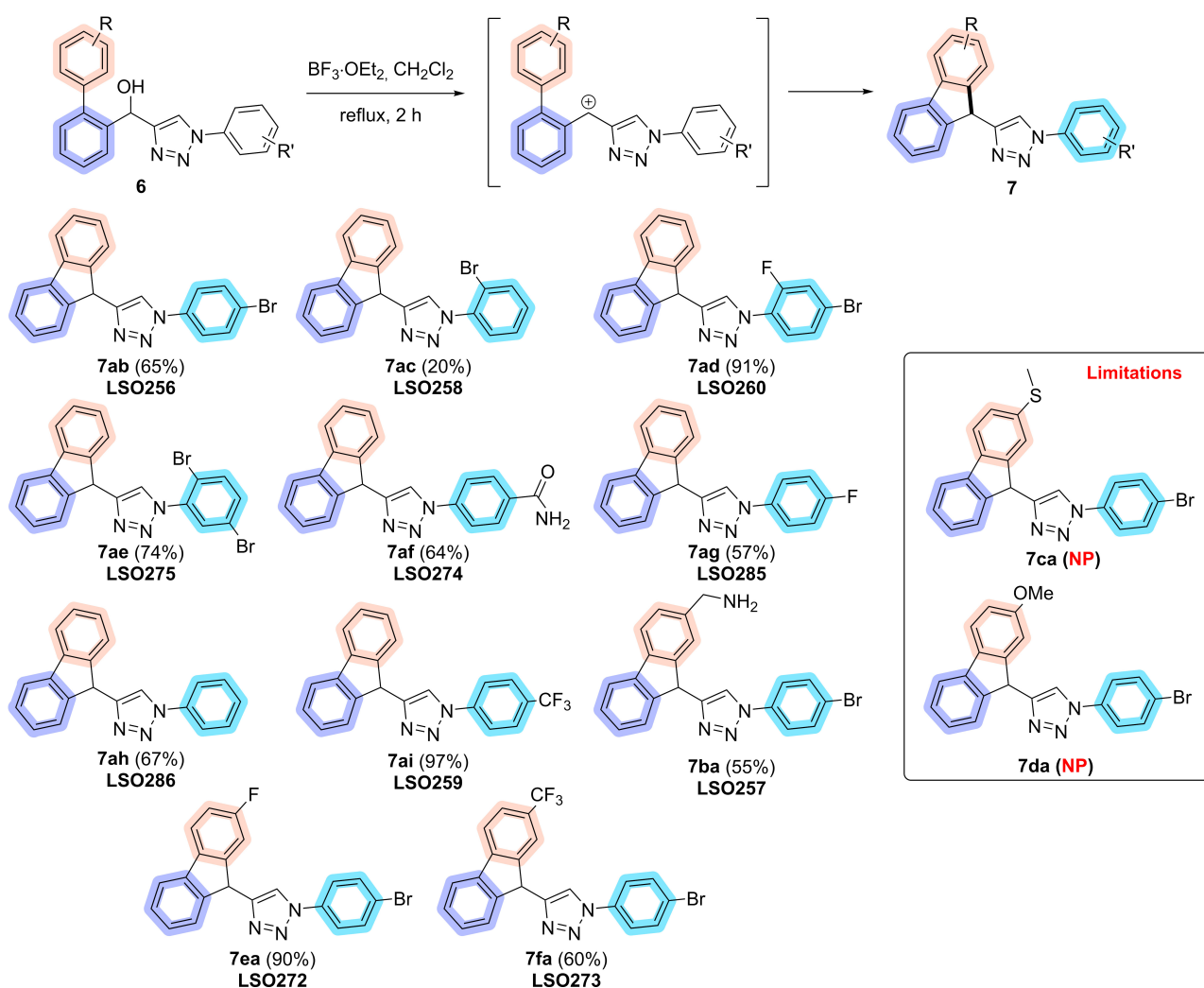

Figure 9. Scope of 9*H*-fluorene-1,2,3-triazoles. NP: no product

The observed variation in yields can be attributed to the position of substituents relative to the cyclization attack site. Optimal yields are achieved when this site has high electronic density, which is enhanced by electron-withdrawing substituents in the meta position and electron-donating substituents in the ortho and para positions. The failure to obtain compounds **7ca** and **7da** is likely due to the presence of

donor groups in the meta position, which reduces the electronic density at the target site, rendering it less reactive and thus deactivating the cyclization process. All products were thoroughly characterized by NMR spectroscopy, while all fluorene-triazoles were analyzed using both NMR and FTIR-ATR (Figures S1–S73).

Biological activity

As previously described, our research group identified the (4-bromophenyl)(1-(4-bromophenyl)-1*H*-1,2,3-triazol-4-yl)methanol and (2-bromophenyl)(1-(4-bromophenyl)-1*H*-1,2,3-triazol-4-yl)methanol, featuring bromine in the aryl ring as important targets for leishmaniasis and cystic fibrosis. However, testing (4-bromophenyl)(1-(4-bromophenyl)-1*H*-1,2,3-triazole-4-yl)methanol (**LSO24**), in these tumor cell lines yielded no so positive results (Table S1).

To identify **LSO24** analogs with enhanced potency against tumor cell lines and assess the influence of flexible ligands biaryl hydroxy-triazoles or scaffolds with conformational rigidity fluorene-1,2,3-triazoles, the cytotoxic effect of the newly synthesized biaryl hydroxy-triazoles and fluorene-triazoles hybrids were evaluated in a single concentration for MGI and in a range of concentration for IC_{50} determination against human cancer cell lines HCT-116 (colorectal cancer), SNB-19 (astrocytoma, glioblastoma multiforme), MDA-MB-231 (triple-negative breast cancer, metastatic) and MOLM-13 (AML). MGI and IC_{50} from all compounds are summarized in Table S1.

The MGI evaluation showed that the compounds **LSO258**, **LSO272**, **LSO276**, **LSO278**, and **LSO281** achieved satisfactory growth inhibition in at least one cell line (Figure 10). Consequently, they were selected for IC_{50} determination in four human cancer cell lines and one non-cancerous human cell line.
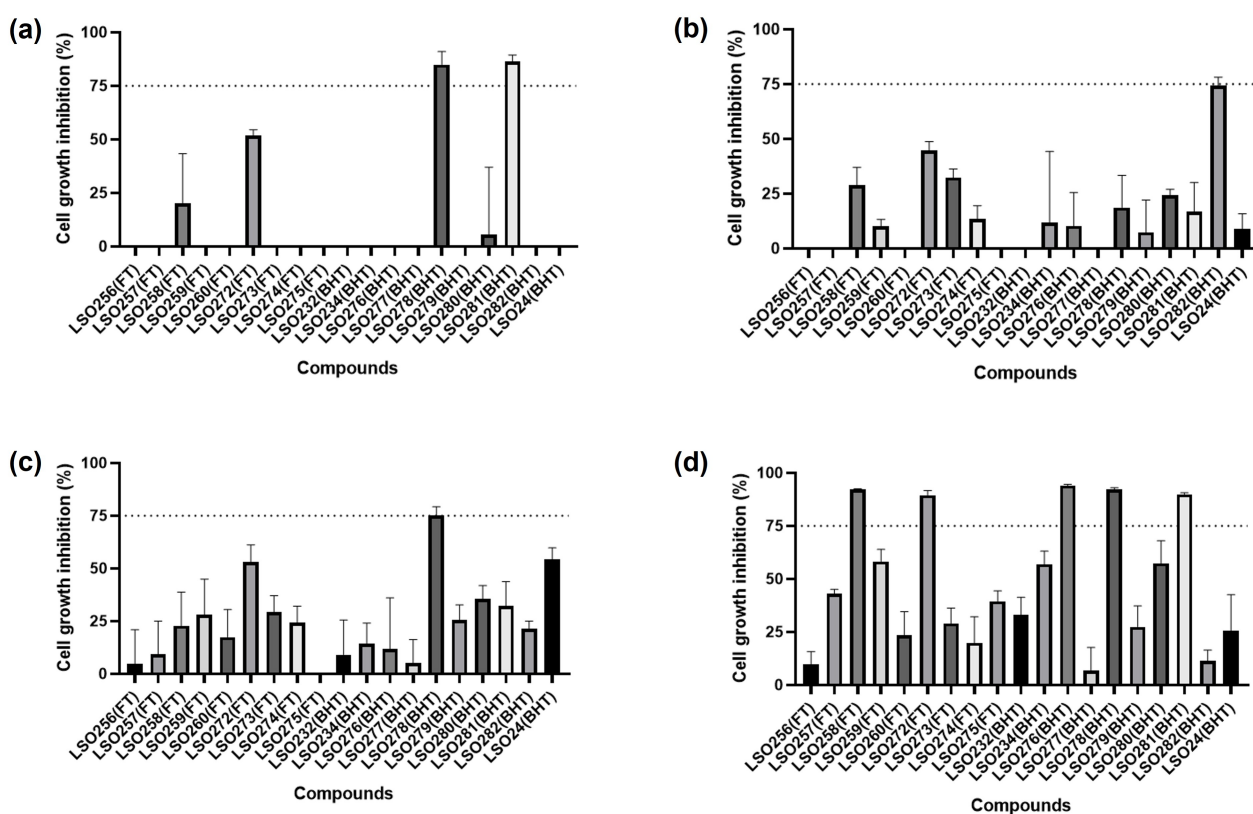
Figure 10. The maximum growth inhibition (MGI) of biaryl hydroxy-triazoles and fluorene-triazoles compounds across a panel of human cancer cell lines after 72 h exposure. (a) HCT-116. (**b**) SNB-19. (**c**) MDA-MB-231. (**d**) MOLM-13

Table 2 presents the IC_{50} evaluation of biaryl hydroxy-triazole and fluorene-triazole compounds against human cancer cell lines. The results indicate that all compounds exhibited an IC_{50} below 50 μM for the MOLM-13 cell line, with **LSO258**, **LSO272**, and **LSO276** demonstrating selectivity for this cell line. The compounds **LS0278** and **LSO281**, both belonging to the biaryl hydroxy-triazoles, were able to achieve an

IC$_{50}$ below 50 μM for more than one cancer cell line. **LSO278** presented a cytotoxicity for the cell line HCT-116 and MDA-MB-231 with IC$_{50}$ values of 23.4 μM and 34.3 μM, respectively. In addition, **LSO281** showed an IC$_{50}$ value of 28.2 μM for the HCT-116 cell line.

Table 2. IC$_{50}$ values (μM) of biaryl hydroxy-triazoles and fluorene-triazoles compounds across a panel of human cell lines after 72 h exposure

Compound	Cell lines				
	HCT-116	**SNB-19**	**MDA-MB-231**	**MOLM-13**	**HEK-293**
LSO258	> 50	> 50	> 50	25.5	> 50
LSO272	> 50	> 50	> 50	12.5	34.5
LSO276	> 50	> 50	> 50	24.8	42.6
LSO278	23.4	> 50	34.3	18.7	20.8
LSO281	28.2	> 50	> 50	22.7	24.7
Doxorubicin	ND	0.8	0.2	ND	0.8
5-Fluorouracil	19.2	ND	ND	ND	6.9
Azacitidine	ND	ND	ND	0.99	> 50

> 50: not able to determine the half-maximal inhibitory concentration (IC$_{50}$) value within the range of concentration tested for this cell line. ND: not determined

Additionally, the compounds were evaluated against the human non-cancer cell line HEK-293 to determine their SI. As shown in Table 3, among the tested compounds, only **LSO258** and **LSO272** exhibited an SI greater than 2 for the MOLM-13 leukemia cell line. In contrast, for the HCT-116, SNB-19, and MDA-MB-231 cell lines, none of the compounds tested showed an SI higher than 1. Notably, **LSO272** demonstrated the highest selectivity, with the lowest IC$_{50}$ value (12.5 μM) for MOLM-13 and an SI of 2.76.

Table 3. Selectivity index of biaryl hydroxy-triazoles and fluorene-triazoles compounds comparing cytotoxicity on tumor cell lines to non-tumor HEK-293 cell line

Compound	Cell lines			
	HCT-116	**SNB-19**	**MDA-MB-231**	**MOLM-13**
LSO258	ND	ND	ND	> 2
LSO272	ND	ND	ND	2.76
LSO276	ND	ND	ND	1.71
LSO278	0.88	ND	0.60	1.11
LSO281	0.87	ND	ND	1.08
Doxorubicin	ND	1	4	ND
5-fluorouracil	0.35	ND	ND	ND
Azacitidine	ND	ND	ND	> 50

ND: not determined

Discussion

Among the fluorene-triazole compounds evaluated, **LSO258** and **LSO272**, both containing bromine at the blue ring exhibited selective cytotoxicity against the MOLM-13 cell line, with IC$_{50}$ values of 25.5 μM and 12.5 μM, respectively. In contrast, the flexible biaryl hydroxy-triazole ligands, **LSO232** and **LSO280**, were inactive. In this case, the rigid scaffolds may minimize the entropic loss associated with the ligand adopting a preferred binding conformation, resulting in enhanced potency, improved selectivity, and reduced potential for drug metabolism [25, 26].

Considering the flexible biaryl hydroxy-triazole ligands, compound **LSO278**, which contains two bromine groups on the blue ring, was the only one to exhibit significant cytotoxicity across three cell lines (HCT-116, MDA-MB-231, and MOLM-13), with IC$_{50}$ values of 23.4 μM, 34.3 μM, and 18.7 μM, respectively. In contrast, the fluorene-triazole compound **LSO275** was inactive even with these two bromine groups, and the conformational rigidity doesn't corroborate the antitumoral activity.

The only instance where both a biaryl hydroxy-triazole (flexible ligand) and a fluorene-triazole (rigid scaffold) demonstrated activity was observed with **LSO258** and **LSO276**, both of which feature bromine in the same position in the blue ring. Compound **LSO276** showed cell line-dependent activity, with an IC_{50} of 24.8 μM in the MOLM-13 acute leukemia cell line and **LSO258** with IC_{50} values of 25.5 μM, both with same potency.

Overall, most of the compounds evaluated in this study were more potent against MOLM-13, even when IC_{50} values were not achieved. For instance, **LSO259**, **LSO234**, and **LSO280** demonstrated an MGI above 55% for MOLM-13, while for cell lines derived from solid tumors, their MGI values were below 35. In addition, most of the compounds evaluated in this study were more potent towards MOLM-13, even those that did not reach an IC_{50} value. For example, **LSO259**, **LSO234**, and **LSO280** displayed an MGI above 55% for MOLM-13, while for the cell lines from solid tumors, only an MGI below 35%.

The MOLM-13 cell line represents a subtype of AML, specifically M5a, characterized by wild-type *TP53* and a mutated *FLT3* gene [52–54]. This FLT3-ITD mutation leads to the constitutive activation of the *FLT3* tyrosine kinase receptor, driving uncontrolled cell proliferation and resistance to apoptosis [55, 56]. As a result, AML patients with this mutation often experience poor survival rates. First-generation tyrosine kinase inhibitors targeting the *FLT3* pathway have been evaluated in clinical trials; however, their low specificity limited their therapeutic efficacy [57, 58]. To overcome this, second-generation *FLT3* inhibitors, such as gilteritinib and quizartinib, were developed and demonstrated significant clinical benefits, leading to their approval for AML treatment in the USA, Japan, and Europe. Nevertheless, treatment resistance remains a challenge, as AML cells can acquire additional mutations in *FLT3* or related genes, ultimately reducing the effectiveness of FLT3 inhibitors [56, 59, 60].

Different studies have shown the antiproliferative effect of 1,2,3-triazoles-hybrids against leukemia cell lines. Ashwini et al. [54] synthesized a series of 1,2-benzisoxazole tethered 1,2,3-triazoles with preeminent anticancer activity in vitro. The lead compound PTB presented IC_{50} ranging from 1–2.5 μM after 96 h exposure in the following cell lines, MOLM-14, MOLM-14 and MV4-11. In another study, novels 1,4-diaryl-1,2,3-triazolo-based ureas compounds were developed as FLT3-ITD inhibitors and tested against cancer cell lines FLT3-ITD dependent (BaF3, MV4-11, and MOM-13) and FLT3-WT cell line. The results showed that different compounds were highly cytotoxic and selective towards FLT3-ITD cell lines compared to the wild-type one. In addition, the molecular docking evaluation indicated that the binding of one of the derivatives was mainly due to the triazole ring [55].

The observed cytotoxicity of bromine-containing fluorene-triazole and biaryl hydroxy-triazole derivatives, particularly **LSO258**, **LSO272**, **LSO276**, and **LSO278**, aligns with the well-established role of bromine in enhancing drug-target interactions through halogen bonding (X-bonding) [56]. Bromine's moderate electronegativity, polarizability, and ability to form directional halogen bonds likely contributed to the increased potency of these compounds, particularly against MOLM-13 cells. Halogen bonds with carbonyl oxygens, amides, and π-stacking with aromatic residues may have improved ligand-protein interactions, enhancing selectivity and binding affinity to biological targets [57, 58]. Furthermore, bromine's lipophilic nature may have facilitated better membrane permeability and cellular uptake, contributing to the observed cytotoxic effects [59].

Additionally, the structural influence of bromine within rigid fluorene-triazole scaffolds suggests that the conformational constraints imposed by this framework may have minimized entropic losses during binding, resulting in more favorable protein-ligand interactions. Interestingly, **LSO278**, a flexible biaryl hydroxy-triazole bearing two bromine atoms, demonstrated broad activity across multiple cancer cell lines, suggesting that in certain cases, enhanced electronic interactions provided by multiple bromine substituents can compensate for flexibility-related entropic penalties. These findings reinforce the importance of bromine in medicinal chemistry, highlighting its potential to fine-tune molecular recognition, optimize pharmacokinetic properties, and enhance cytotoxicity in drug discovery efforts [60, 61].

In conclusion, we successfully synthesized 13 new biaryl hydroxy-1,2,3-triazoles using a one-pot reaction that eliminated the need for isolating intermediates, achieving yields ranging from 16% to 89%. These triazoles served as precursors for 9H-fluorene-triazole hybrids, resulting in the formation of novel compounds with yields between 20% and 97%. The synthesized structures demonstrated significant potential for inhibiting the growth of several cancer cell lines. Among the compounds evaluated, most exhibited higher potency against MOLM-1, with **LSO258**, **LSO272**, **LSO276**, and **LSO278** showing IC$_{50}$ values of 25.5, 12.5, 24.8, and 18.7 μM, respectively. Notably, **LSO278** displayed versatility, exhibiting additional activity against HCT-116 (IC$_{50}$ = 23.4 μM) and MDA-MB-231 (IC$_{50}$ = 34.3 μM). While a direct correlation between flexible ligands and rigid scaffolds could not be established, the presence of a triazole moiety and bromine substitution on the blue ring (derived from aryl azide) consistently emerged as key features, as all active compounds shared this structure.

Abbreviations

AML: acute myeloid leukemia

CuAAC: copper-catalyzed alkyne-azide cycloaddition

DMF-DMA: *N,N*-dimethylformamide dimethyl acetal

EACA: enaminone-azide cycloaddition

EtOAc: ethyl acetate

IC$_{50}$: half-maximal inhibitory concentration

InhA: NADH-dependent 2-*trans*-enoyl-acyl carrier protein reductase

MGI: maximum growth inhibition

MTT: 3-(4,5-dimethyl-2-thiazolyl)-2,5-diphenyl-2H-tetrazolium bromide

SI: selectivity index

Supplementary materials

The supplementary figures for this article are available at: https://www.explorationpub.com/uploads/Article/file/1008107_sup_1.pdf. The supplementary table for this article is available at: https://www.explorationpub.com/uploads/Article/file/1008107_sup_2.pdf.

Declarations

Author contributions

DCZ: Writing—original draft, Investigation, Data curation. MFMFA: Writing—review & editing, Investigation, Data curation. MSR and RdSB: Investigation. JdBVN: Writing—original draft, Investigation. CdÓP: Validation, Supervision, Funding acquisition. CDB: Conceptualization, Validation, Writing—review & editing, Supervision, Funding acquisition. All authors read and approved the submitted version.

Conflicts of interest

The authors declare that they have no conflicts of interest.

Ethical approval

Not applicable.

Consent to participate

Not applicable.

Publisher's note

Open Exploration maintains a neutral stance on jurisdictional claims in published institutional affiliations and maps. All opinions expressed in this article are the personal views of the author(s) and do not represent the stance of the editorial team or the publisher.

References

1. Bray F, Laversanne M, Weiderpass E, Soerjomataram I. The ever-increasing importance of cancer as a leading cause of premature death worldwide. Cancer. 2021;127:3029–30. [DOI] [PubMed]

2. World Health Organization (WHO). Global Health Estimates 2021: Deaths by Cause, Age, Sex, by Country and by Region, 2000-2021 [Internet]. Geneva, World Health Organization; c2025 [cited 2024 Dec 14]. Available from: https://www.who.int/data/gho/data/themes/mortality-and-global-health-estimates/ghe-leading-causes-of-death

3. Sung H, Ferlay J, Siegel RL, Laversanne M, Soerjomataram I, Jemal A, et al. Global Cancer Statistics 2020: GLOBOCAN Estimates of Incidence and Mortality Worldwide for 36 Cancers in 185 Countries. CA Cancer J Clin. 2021;71:209–49. [DOI] [PubMed]

4. Khan SU, Fatima K, Aisha S, Malik F. Unveiling the mechanisms and challenges of cancer drug resistance. Cell Commun Signal. 2024;22:109. [DOI] [PubMed] [PMC]

5. Desbats MA, Giacomini I, Prayer-Galetti T, Montopoli M. Metabolic plasticity in chemotherapy resistance. Front Oncol. 2020;10:281. [DOI]

6. De Conti G, Dias MH, Bernards R. Fighting Drug Resistance through the Targeting of Drug-Tolerant Persister Cells. Cancers (Basel). 2021;13:1118. [DOI] [PubMed] [PMC]

7. Azim HA Jr, de Azambuja E, Colozza M, Bines J, Piccart MJ. Long-term toxic effects of adjuvant chemotherapy in breast cancer. Ann Oncol. 2011;22:1939–47. [DOI] [PubMed]

8. Nguyen SM, Pham AT, Nguyen LM, Cai H, Tran TV, Shu XO, et al. Chemotherapy-Induced Toxicities and Their Associations with Clinical and Non-Clinical Factors among Breast Cancer Patients in Vietnam. Curr Oncol. 2022;29:8269–84. [DOI] [PubMed] [PMC]

9. Zhao S, Liu J, Lv Z, Zhang G, Xu Z. Recent updates on 1,2,3-triazole-containing hybrids with *in vivo* therapeutic potential against cancers: A mini-review. Eur J Med Chem. 2023;251:115254. [DOI] [PubMed]

10. Xu Z, Zhao SJ, Liu Y. 1,2,3-Triazole-containing hybrids as potential anticancer agents: Current developments, action mechanisms and structure-activity relationships. Eur J Med Chem. 2019;183: 111700. [DOI] [PubMed]

11. Guan Q, Gao Z, Chen Y, Guo C, Chen Y, Sun H. Structural modification strategies of triazoles in anticancer drug development. Eur J Med Chem. 2024;275:116578. [DOI] [PubMed]

12. Kislukhin AA, Hong VP, Breitenkamp KE, Finn MG. Relative performance of alkynes in copper-catalyzed azide–alkyne cycloaddition. Bioconjug Chem. 2013;24:684–9. [DOI] [PubMed] [PMC]

13. Azevedo MFMF, Zeitune DC, de Farias RL, Junior ENC, Bacalhau M, Amaral MD, et al. Direct access of 4-acyl-1,2,3-triazoles from acetophenones: A synthetic shortcut for novel p.Phe508del-CFTR traffic correctors. J Mol Struct. 2025;1321:139897. [DOI]

14. Almeida-Souza F, da Silva VD, Taniwaki NN, Hardoim DJ, Mendonça Filho AR, Moreira WFF, et al. Nitric Oxide Induction in Peritoneal Macrophages by a 1,2,3-Triazole Derivative Improves Its Efficacy upon *Leishmania amazonensisIn Vitro* Infection. J Med Chem. 2021;64:12691–704. [DOI] [PubMed]

15. Cirne-Santos C, Batista RRS, Souza Barros C, Azevedo MFMF, Ronconi CM, Buarque CD, et al. In vitro study of the inhibitory potential of hydroxy-1,2,3-triazoles on the replication of ZIKA and chikungunya arboviruses. Results Chem. 2024;8:101589. [DOI]

16. Belfield KD, Yao S, Bondar MV. Two-photon Absorbing Photonic Materials: From Fundamentals to Applications. In: Marder SR, Lee KS, editors. Photoresponsive Polymers I. Heidelberg: Springer; 2008. pp. 97–156.

17. Anthony JE. Functionalized acenes and heteroacenes for organic electronics. Chem Rev. 2006;106: 5028–48. [DOI] [PubMed]

18. Inganäs O, Zhang F, Andersson MR. Alternating polyfluorenes collect solar light in polymer photovoltaics. Acc Chem Res. 2009;42:1731–9. [DOI] [PubMed]

19. Wang L, Dong B, Ge R, Jiang F, Xu J. Fluorene-Based Two-Dimensional Covalent Organic Framework with Thermoelectric Properties through Doping. ACS Appl Mater Interfaces. 2017;9:7108–14. [DOI] [PubMed]

20. Nakabayashi K, Imai T, Fu MC, Ando S, Higashihara T, Ueda M. Poly(phenylene thioether)s with Fluorene-Based Cardo Structure toward High Transparency, High Refractive Index, and Low Birefringence. Macromolecules. 2016;49:5849–56. [DOI]

21. Morgan LR, Thangaraj K, LeBlanc B, Rodgers A, Wolford LT, Hooper CL, et al. Design, synthesis, and anticancer properties of 4,4'-dihydroxybenzophenone-2,4-dinitrophenylhydrazone and analogues. J Med Chem. 2003;46:4552–63. [DOI] [PubMed]

22. Fan C, Wang W, Wang Y, Qin G, Zhao W. Chemical constituents from *Dendrobium densiflorum*. Phytochemistry. 2001;57:1255–8. [DOI] [PubMed]

23. Tierney MT, Grinstaff MW. Synthesis and characterization of fluorenone-, anthraquinone-, and phenothiazine-labeled oligodeoxynucleotides: 5'-probes for DNA redox chemistry. J Org Chem. 2000; 65:5355–9. [DOI] [PubMed]

24. Saikawa Y, Hashimoto K, Nakata M, Yoshihara M, Nagai K, Ida M, et al. The red sweat of the hippopotamus. Nature. 2004;429:363. [DOI] [PubMed]

25. Fang Z, Song Y, Zhan P, Zhang Q, Liu X. Conformational restriction: an effective tactic in 'follow-on'-based drug discovery. Future Med Chem. 2014;6:885–901. [DOI] [PubMed]

26. Lawson ADG, MacCoss M, Heer JP. Importance of Rigidity in Designing Small Molecule Drugs To Tackle Protein–Protein Interactions (PPIs) through Stabilization of Desired Conformers. J Med Chem. 2018; 61:4283–9. [DOI] [PubMed]

27. Zhu Y, Guang S, Su X, Xu H, Xu D. Dependence of the intramolecular charge transfer on molecular structure in triazole bridge-linked optical materials. Dyes Pigm. 2013;97:175–83. [DOI]

28. Denneval C, Moldovan O, Baudequin C, Achelle S, Baldeck P, Plé N, et al. Synthesis and Photophysical Properties of Push–Pull Structures Incorporating Diazines as Attracting Part with a Fluorene Core. European J Org Chem. 2013;2013:5591–602. [DOI]

29. Brunel D, Dumur F. Recent advances in organic dyes and fluorophores comprising a 1,2,3-triazole moiety. New J Chem. 2020;44:3546–61. [DOI]

30. van Steenis DJ, David OR, van Strijdonck GP, van Maarseveen JH, Reek JN. Click-chemistry as an efficient synthetic tool for the preparation of novel conjugated polymers. Chem Commun (Camb). 2005:4333–5. [DOI] [PubMed]

31. Qin A, Jim CKW, Lam JWY, Sun J, Tang BZ. Synthesis of a hyperbranched poly(aroylarylene) containing triazole and fluorene functionalities by click chemistry and metal-free, regioselective polycyclotrimerization. Chin J Polym Sci. 2009;27:145. [DOI]

32. Hong SW, Hwang GT. Photophysical Study of 2-Fluorenyl-1,2,3-Triazole-labeled 2′-Deoxyuridine and Its Oligonucleotide. Bull Korean Chem Soc. 2018;39:78–83. [DOI]

33. Sirivolu VR, Vernekar SK, Ilina T, Myshakina NS, Parniak MA, Wang Z. Clicking 3'-azidothymidine into novel potent inhibitors of human immunodeficiency virus. J Med Chem. 2013;56:8765–80. [DOI] [PubMed] [PMC]

34. Yarchoan R, Mitsuya H, Myers CE, Broder S. Clinical pharmacology of 3'-azido-2',3'-dideoxythymidine (zidovudine) and related dideoxynucleosides. N Engl J Med. 1989;321:726–38. [DOI] [PubMed]

35. KohPark KH, Jung HM, Lee TW, Kang SK. Synthesis and Structure of Benzotriazolyl Fluorenes. Bull Korean Chem Soc. 2010;31:984–8. [DOI]

36. Yang YD, Tokunaga E, Akiyama H, Saito N, Shibata N. Bis(pentafluorosulfanyl)phenyl azide as an expeditious tool for click chemistry toward antitumor pharmaceuticals. ChemMedChem. 2014;9: 913–7. [DOI] [PubMed]

37. Suresh A, Srinivasarao S, Agnieszka N, Ewa AK, Alvala M, Lherbet C, et al. Design and synthesis of 9*H*-fluorenone based 1,2,3-triazole analogues as *Mycobacterium tuberculosis* InhA inhibitors. Chem Biol Drug Des. 2018;91:1078–86. [DOI] [PubMed]

38. da Silva VD, Silva RR, Gonçalves Neto J, López-Corcuera B, Guimarães MZ, Noël F, et al. New α-Hydroxy-1,2,3-triazoles and 9*H*-Fluorenes-1,2,3-triazoles: Synthesis and Evaluation as Glycine Transporter 1 Inhibitors. J Braz Chem Soc. 2020;31:1258–69. [DOI]

39. Carmichael J, DeGraff WG, Gazdar AF, Minna JD, Mitchell JB. Evaluation of a tetrazolium-based semiautomated colorimetric assay: assessment of chemosensitivity testing. Cancer Res. 1987;47: 936–42. [PubMed]

40. Mosmann T. Rapid colorimetric assay for cellular growth and survival: application to proliferation and cytotoxicity assays. J Immunol Methods. 1983;65:55–63. [DOI] [PubMed]

41. Peña-Morán OA, Villarreal ML, Álvarez-Berber L, Meneses-Acosta A, Rodríguez-López V. Cytotoxicity, Post-Treatment Recovery, and Selectivity Analysis of Naturally Occurring Podophyllotoxins from *Bursera fagaroides* var. *fagaroides* on Breast Cancer Cell Lines. Molecules. 2016;21:1013. [DOI] [PubMed] [PMC]

42. Widiandani T, Tandian T, Zufar BD, Suryadi A, Purwanto BT, Hardjono S, et al. In vitro study of pinostrobin propionate and pinostrobin butyrate: Cytotoxic activity against breast cancer cell T47D and its selectivity index. J Public Health Afr. 2023;14:2516. [DOI] [PubMed] [PMC]

43. Hoffmann I, Blumenröder B, Onodi neé Thumann S, Dommera S, Schatz J. Suzuki cross-coupling in aqueous media. Green Chem. 2015;17:3844–57. [DOI]

44. Zhou X, Guo X, Jian F, Wei G. Highly Efficient Method for Suzuki Reactions in Aqueous Media. ACS Omega. 2018;3:4418–22. [DOI] [PubMed] [PMC]

45. Suzuki A. Organoborane coupling reactions (Suzuki coupling). Proc Jpn Acad, Ser B. 2004;80:359–71. [DOI]

46. Chemler SR, Trauner D, Danishefsky SJ. The *B*-Alkyl Suzuki–Miyaura Cross-Coupling Reaction: Development, Mechanistic Study, and Applications in Natural Product Synthesis. Angew Chem Int Ed Engl. 2001;40:4544–68. [DOI] [PubMed]

47. Thomas J, Goyvaerts V, Liekens S, Dehaen W. Metal-Free Route for the Synthesis of 4-Acyl-1,2,3-Triazoles from Readily Available Building Blocks. Chemistry. 2016;22:9966–70. [DOI] [PubMed]

48.   Gaspar FV, Azevedo MFMF, Carneiro LSA, Ribeiro SB, Esteves PM, Buarque CD. 1,3-Dipolar cycloaddition reactions of enaminones and azides: Synthesis of 4-acyl-1,2,3-triazoles and mechanistic studies. Tetrahedron. 2022;120:132856. [DOI]

49.   de Andrade VSC, de Mattos MCS. A abordagem telescópica como ferramenta da química verde. Quim Nova. 2021;44:912–8. [DOI]

50.   Zhou J, Yang W, Wang B, Ren H. Friedel–Crafts Arylation for the Formation of C_{sp}^2—C_{sp}^2 Bonds: A Route to Unsymmetrical and Functionalized Polycyclic Aromatic Hydrocarbons from Aryl Triazenes. Angew Chem Int Ed Engl. 2012;51:12293–7. [DOI] [PubMed]

51.   Rueping M, Nachtsheim BJ. A review of new developments in the Friedel–Crafts alkylation – From green chemistry to asymmetric catalysis. Beilstein J Org Chem. 2010;6:6. [DOI] [PubMed] [PMC]

52.   Kancharla P, Dodean RA, Li Y, Kelly JX. Boron Trifluoride Etherate Promoted Microwave-Assisted Synthesis of Antimalarial Acridones. RSC Adv. 2019;9:42284–93. [DOI] [PubMed] [PMC]

53.   Killander D, Sterner O. Reagent-Controlled Cyclization–Deprotection Reaction to Yield either Fluorenes or Benzochromenes. European J Org Chem. 2014;2014:6507–12. [DOI]

54.   Ashwini N, Garg M, Mohan CD, Fuchs JE, Rangappa S, Anusha S, et al. Synthesis of 1,2-benzisoxazole tethered 1,2,3-triazoles that exhibit anticancer activity in acute myeloid leukemia cell lines by inhibiting histone deacetylases, and inducing p21 and tubulin acetylation. Bioorg Med Chem. 2015;23: 6157–65. [DOI] [PubMed]

55.   Liu J, Wang Y, Chen C, Tu Z, Zhu S, Zhou F, et al. Identification and Development of 1,4-Diaryl-1,2,3-triazolo-Based Ureas as Novel FLT3 Inhibitors. ACS Med Chem Lett. 2020;11:1567–72. [DOI] [PubMed] [PMC]

56.   Scholfield MR, Zanden CM, Carter M, Ho PS. Halogen bonding (X-bonding): a biological perspective. Protein Sci. 2013;22:139–52. [DOI] [PubMed] [PMC]

57.   Carter M, Rappé AK, Ho PS. Scalable Anisotropic Shape and Electrostatic Models for Biological Bromine Halogen Bonds. J Chem Theory Comput. 2012;8:2461–73. [DOI] [PubMed]

58.   Hernandes MZ, Cavalcanti SM, Moreira DR, de Azevedo Junior WF, Leite AC. Halogen atoms in the modern medicinal chemistry: hints for the drug design. Curr Drug Targets. 2010;11:303–14. [DOI] [PubMed]

59.   Lu Y, Liu Y, Xu Z, Li H, Liu H, Zhu W. Halogen bonding for rational drug design and new drug discovery. Expert Opin Drug Discov. 2012;7:375–83. [DOI] [PubMed]

60.   Lu Y, Shi T, Wang Y, Yang H, Yan X, Luo X, et al. Halogen Bonding—A Novel Interaction for Rational Drug Design? J Med Chem. 2009;52:2854–62. [DOI] [PubMed]

61.   Cavallo G, Metrangolo P, Milani R, Pilati T, Priimagi A, Resnati G, et al. The Halogen Bond. Chem Rev. 2016;116:2478–601. [DOI] [PubMed] [PMC]